RESEARCH ARTICLE OPEN ACCESS

Parallel Networks to Predict TIMP and Protease Cell Activity of Nucleus Pulposus Cells Exposed and Not Exposed to Pro-Inflammatory Cytokines

L. Baumgartner | S. Witta | J. Noailly

Biomechanics and Mechanobiology, BCN MedTech, Department of Engineering, Pompeu Fabra University, Barcelona, Spain

Correspondence: J. Noailly (jerome.noailly@upf.edu)

Received: 9 September 2024 | **Revised:** 27 January 2025 | **Accepted:** 2 February 2025

Funding: This work was supported by HORIZON EUROPE European Research Council (ERC-2021-CoG-O-Health-101044828).

Keywords: cell nutrition | intervertebral disc | mechanotransduction | mRNA expression | network modeling | parallel networks | pro-inflammatory cytokines | proteases | structural proteins | TIMP

ABSTRACT

Background: Intervertebral disc (IVD) degeneration is characterized by a disruption of the balance between anabolic and catabolic cellular processes. Within the nucleus pulposus (NP), this involves increased levels of the pro-inflammatory cytokines interleukin 1beta (IL1B) and tumor necrosis factor (TNF) and an upregulation of the protease families matrix metalloproteinase (MMP) and a disintegrin and metalloproteinase with thrombospondin motifs (ADAMTS). Primary inhibitors of these proteases are the tissue inhibitors of matrix metalloproteinases (TIMP). This work aims at contributing to a better understanding of the dynamics among proteases, TIMP, and pro-inflammatory cytokines within the complex, multifactorial environment of the NP.

Methods: The Parallel Network (PN)-Methodology was used to estimate relative mRNA expressions of TIMP1–3, MMP3, and ADAMTS4 for five simulated human activities: walking, sitting, jogging, hiking with 20 kg extra weight, and exposure to high vibration. Simulations were executed for nutrient conditions in non- and early-degenerated IVD approximations. To estimate the impact of cytokines, the PN-Methodology inferred relative protein levels for IL1B and TNF, reintegrated as secondary stimuli into the network.

Results: TIMP1 and TIMP2 expressions were found to be overall lower than TIMP3 expression. In the absence of pro-inflammatory cytokines, MMP3 and/or ADAMTS4 expressions were strongly downregulated in all conditions but vibration and hiking with extra weight. Pro-inflammatory cytokine exposure resulted in an impaired inhibition of MMP3, rather than of ADAMTS4, progressively rising with increasing nutrient deprivation. TNF mRNA was less expressed than IL1B. However, at the protein level, TNF was mainly responsible for the catabolic shift in the simulated pro-inflammatory environment. Overall, results agreed with previous experimental findings.

Conclusions: The PN-Methodology successfully allowed the exploration of the relative dynamics of TIMP and protease regulations in different mechanical, nutritional, and inflammatory environments in the NP. It shall stand as a comprehensive tool to integrate in vitro model results in IVD research and approximate NP cell activities in complex multifactorial environments.

1 | Introduction

Low back pain is the leading cause of disability worldwide, presenting both an economic and epidemiological burden [1, 2]. It affects up to 85% of people [3], predominantly individuals in middle to old age, imposing severe restrictions in social and physical capacity and importantly affecting mental health [4].

The onset of low back pain is strongly correlated with intervertebral disc (IVD) degeneration (IDD) [4]. IDD is characterized by a disruption of the balance between catabolic and anabolic protein secretion, which increases the presence of proteases that degrade the IVD extracellular matrix [5–7]. Thereby, matrix metalloproteinase-3 (MMP3) and a disintegrin and metalloproteinase with thrombospondin motifs-4 (ADAMTS4) are key proteases in IDD, correlating with increasing degeneration grade [5–9].

The main inhibitors of proteases are the tissue inhibitor of matrix metalloproteinases (TIMP). Four TIMP are known, out of which TIMP1–3 are most commonly investigated. TIMP3 is the only member of the TIMP family bound to the extracellular matrix [10]. The inhibition of proteases by TIMP occurs through an interaction with the active cleavage site of the proteases in a 1:1 stoichiometric ratio by forming a non-covalent complex [11–13]. The N-terminal domain of TIMP is assumed to play a critical role in the binding specificities [11]. TIMP1 and TIMP2 have a high binding affinity to MMP3 [11, 14], while TIMP3 shows greater specificity for ADAMTS4 [15]. Beyond the aforementioned details of interactions, the effective control and role of TIMP to maintain the integrity of the IVD in a multifactorial environment, however, remain poorly apprehended and were, therefore, tackled in this work.

In addition to an increase in protease activity, pro-inflammatory cytokine expression increases during IDD. Especially interleukin 1 beta (IL1B) and tumor necrosis factor (TNF) have been shown to be elevated in degenerated discs [16, 17]. IL1B treatment in non-degenerated nucleus pulposus (NP) cells led to upregulated gene expression of key catabolic proteins including MMP3 and ADAMTS4 [5]. Elevated TNF levels were associated with non-recoverable catabolic shifts in the IVD [18]. However, the role of pro-inflammatory cytokines in the dual regulation of proteases and TIMP has not yet been elucidated.

According to experimental models, nutritional and mechanical extrinsic stimulations are believed to largely influence IVD cells [9]. As the IVD is the largest avascular structure within the human body [19] cell nutrition depends on the diffusion of nutrients from the capillaries located at the Cartilage Endplates [20]. This creates steep gradients of nutrients (oxygen, glucose, pH), resulting in low glucose and oxygen concentrations and low pH around the mid transverse plane of the NP [20]. Additionally, human movement activities cause the IVD to be dynamically exposed to a variety of mechanical loads, translated into varying intradiscal pressures (magnitude) and frequencies into the NP [21]. Despite extensive studies evaluating the effect of key nutritional (pH, glucose) and mechanical (magnitude, frequency) stimuli on gene expression of TIMP and proteases [22–26], insight on the combined effect of regulatory stimuli on NP cell activity (CA) is limited. Furthermore, it is necessary to apprehend the role of pro-inflammatory cytokines in multifactorial environments. While experimental research remains time and cost intensive, in silico methods to approximate dynamics at a (multi-)cellular level provide a promising approach.

A methodology was recently proposed to simulate CA regulated by multifactorial stimulus environments, which was mathematically represented as simultaneous ongoing actions in parallel networks (PN) [27]. This method combines experimental data about cell responses to varying stimulus doses; it allows to estimate effective CA directly at the (multi-)cellular level while considering intracellular regulations as a "black box." The PN-Methodology also allows automatically switching the nature of a stimulus (i.e., activating or inhibiting), depending on the dose of this stimulus, as informed by experimental models.

Hence, the objective of this work is to investigate the dynamics of TIMP1–3, MMP3, and ADAMTS4 in response to complex microenvironmental stimuli, with and without TNF and IL1B proteins. To this end, the PN-Methodology was further leveraged regarding mathematical estimations of mRNA–protein dynamics.

2 | Materials and Methods

2.1 | Overview of the Simulated Network

mRNA expressions of TIMP1, TIMP2, TIMP3, MMP3, ADAMTS4, IL1B, and TNF were estimated based on user-defined levels of key nutritional and mechanical stimuli, within ranges of stimulus doses defined in the literature (Figure 1). Stimulus doses were set to simulate five human activities: sitting, walking, hiking with 20 kg extra weight, and exposure to vibration. Each activity was simulated for three nutritional conditions, covering optimal, critical, and early degenerated cell environments.

mRNA levels of IL1B and TNF were translated into protein levels and refed into the PN-System as secondary stimuli to obtain TIMP1, TIMP2, TIMP3, MMP3, and ADAMTS4 of cells exposed to a pro-inflammatory environment (Figure 1).

As opposed to nutritional stimuli that define a baseline activation and are, therefore, always activating (see [27] for more information), the nature of mechanical stimuli (magnitude, frequency) depends on the stimulus dose. The effect of pro-inflammatory cytokines was assumed to be either only activating or only inhibiting (Figure 1).

2.2 | Overview of the PN-Methodology

The PN-Methodology [27] interprets each CA as an interdependent parallel ongoing action of a cell. Thereby, each CA (here mRNA expression) is determined by combinations of the key nutritional stimuli glucose, pH, magnitude and frequency and reflect one PN. Accordingly, many CA are reflected as many relatively small feedforward PN. The relationship between one stimulus with one targeted mRNA expression is called S-CA relationship and is determined by the product of the two variables θ and x. Both are sensitive to the specific stimulus (subscript S) and cell activity (superscript CA) and therefore specified as x_S^{CA} and θ_S^{CA}, respectively.

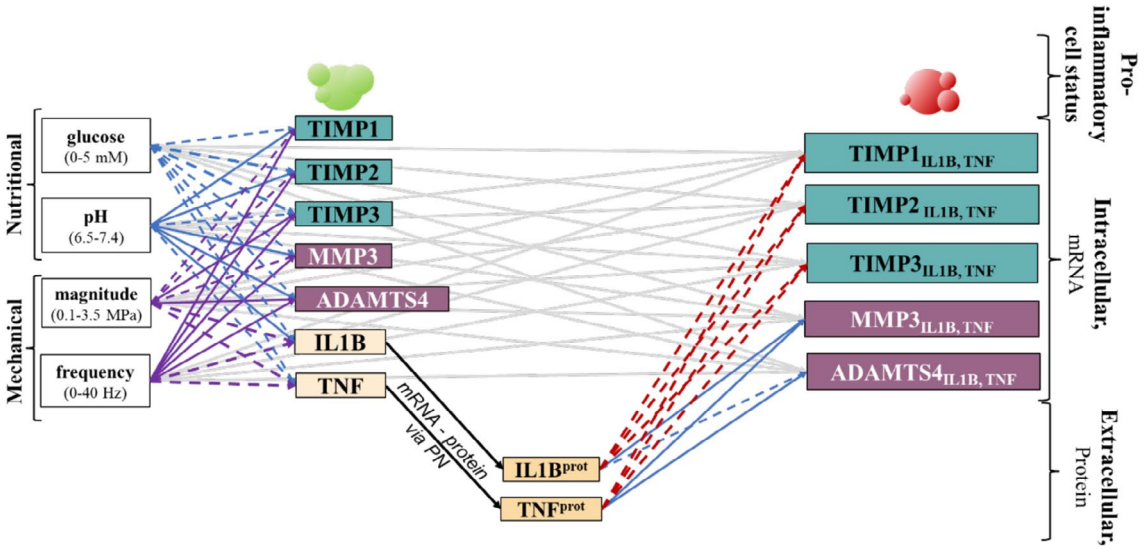

FIGURE 1 | Overview of the simulated environment. The PN-Methodology was used to estimate the relative mRNA expressions of the targeted proteins MMP3, ADAMTS4, TIMP1, TIMP2, and TIMP3 exposed and not exposed to pro-inflammatory cytokines. For cells not exposed to pro-inflammatory cytokines (green colored cells), mRNA expressions were based on glucose concentration, pH, load magnitude, and load frequency, while cells exposed to pro-inflammatory cytokines (red colored cells) additionally obtained input from IL1B and TNF proteins (prot). The nature of the links may be generally activating (blue), generally inhibiting (red), or depending on the stimulus dose (purple). Links reported to be statistically significant in the experimental literature are marked with a continuous line; those reported to be nonsignificant are reflected by a dashed line. Gray S-CA relationships have the same value than their counterpart in the cytokine-free environment. Extracellular: The PN-methodological concept was used to estimate protein levels of IL1B and TNF, required to estimate a pro-inflammatory environment.

x_S^{CA} approximates the sensitivity of a mRNA expression to a given stimulus dose through a function. This function is based on discrete values from the literature and assigns a CA to a stimulus dose. If a stimulus is only activating or inhibiting, the CA ranges between 0 (minimal mRNA expression at a given stimulus dose) and 1 (maximal mRNA expression at a given stimulus dose). If the nature of a CA is dose-dependent, it ranges between −1 and 1. Thereby, positive and negative values reflect an activating and inhibiting effect, respectively, as previously explained [27] (see Figure 3, Section 3). The more the CA tends to 1 the higher is its activating effect, and the more the CA tends to −1, the higher is its inhibiting effect.

θ_S^{CA} is a (real) number bigger than 0 and maximum 1. It reflects the impact of a stimulus on a given CA and is called "weighting factor." It is derived from the maximal change in mRNA expression, optimally directly calculated from the experimental measurements used to determine x_S^{CA}. The in-depth pipeline to obtain θ_S^{CA} [28] and x_S^{CA} [29] were provided before and visualized in Figure 2.

To describe the network given in Figure 1, 38 links (S-CA relationships) need to be specified, each in terms of the sensitivity of a CA to varying stimulus dose (x_S^{CA}) and in terms of the overall impact this stimulus might have on a CA (θ_S^{CA}).

Whenever possible, CA should be estimated for physiologically relevant stimulus doses. For the NP, glucose concentrations range between 0 and 5 mM [30], pH ranges between 6.5 and 7.4 [23] and magnitude varies between 0.1 and 3.5 MPa [21, 31]. For frequency, a relevant range for a set of human daily activities was chosen, starting from 0 Hz (static) to 40 Hz to simulate whole body vibrations, such as caused by vehicle engines.

In terms of cell type, human (non-degenerated) cells were prioritized over bovine cells. Otherwise, *in vitro* work with rat cells was used (Appendix S1). 3D cell cultures were preferred over 2D cell cultures. As NP cells change their biological activity as they progress from immature to mature, mature NP cells were preferred.

The activity of each PN was calculated with the PN-Equation (Equation 1) [27, 28] that determines the individual activation and strength of each PN within the PN-System. Briefly: the PN-Equation consists of an activating (α) and an inhibiting (β) portion. The activating portion consists of two terms; in its first term, it considers all the activating weighting factors of the PN-System $\left(\theta_\alpha\right)$. This includes the potentially activating contribution of dose-dependent stimuli. The first activating term is then multiplied with the activating S-CA relationships of the actual PN $\left(\theta_{S,\alpha}^{CA} x_{S,\alpha}^{CA}\right)$. This gives the weight of the tackled PN in the light of the whole PN-System. The inhibiting portion consists of three terms and is calculated independently from the activating term. The first inhibiting term determines the relative strength of the inhibitors for this mRNA. The second term includes all the inhibiting weighting factors for a given mRNA, independently of the CS. The third inhibiting term, eventually, calculates the actual inhibiting S-CA relationship of this PN.

$$\omega_{CA,CS} = \left(\left(\frac{1+\sum\theta_\alpha}{\sum\theta_\alpha}\right)\left(\frac{\sum\theta_{S,\alpha}^{CA}x_{S,\alpha}^{CA}}{1+\sum\theta_{S,\alpha}^{CA}x_{S,\alpha}^{CA}}\right)\right) \cdot\left(1-\left(\left(\frac{\sum\theta_{S,\beta}^{CA}}{\sum\theta_{S,\alpha}^{CA}+\sum\theta_{S,\beta}^{CA}}\right)\left(\left(\frac{1+\sum\theta_\beta^{CA}}{\sum\theta_\beta^{CA}}\right)\left(\frac{\sum\theta_{S,\beta}^{CA}x_{S,\beta}^{CA}}{1+\sum\theta_{S,\beta}^{CA}x_{S,\beta}^{CA}}\right)\right)\right)\right) \quad (1)$$

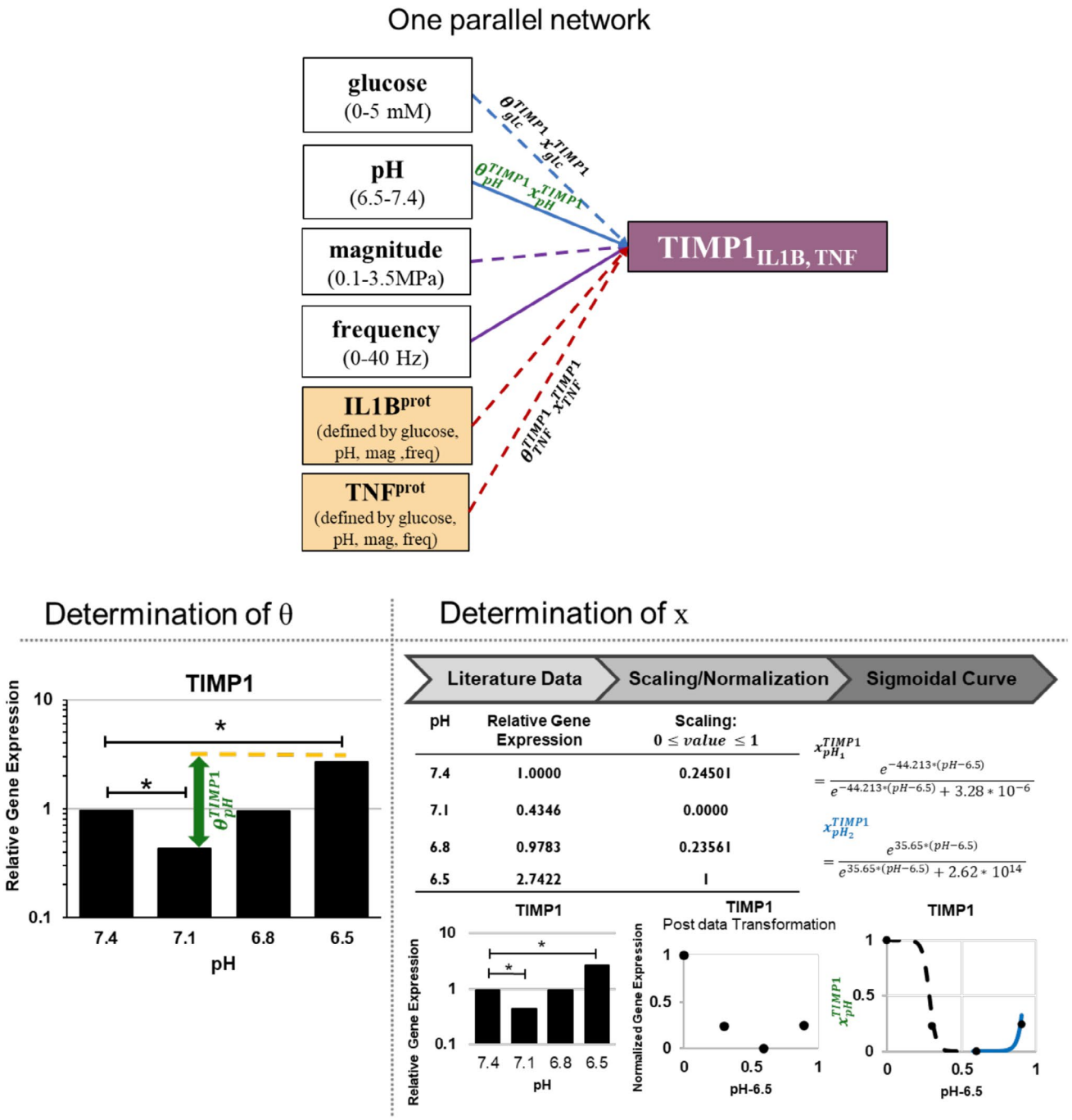

FIGURE 2 | Top: One parallel network of TIMP1 for cells exposed to pro-inflammatory cytokines (see also Figure 1). Stimulus-cell activity (S-CA) relationships are exemplarily mentioned for glucose (glc)-TIMP1, TNF-TIMP1, and pH-TIMP1 (green). Below: Data extraction for pH-TIMP1. Determination of θ: Experimental data about TIMP1 mRNA expression at different pH (modified from [23]). θ reflects the highest change in relative gene expression. Determination of x: Relative gene expression at pH 7.4, 7.1, 6.8, and 6.5 were normalized to fit continuous sigmoidal functions to approximate a continuous cell activity for TIMP1 mRNA expression throughout a physiological range of pH. mag: magnitude; freq: frequency.

To explicitly assign S-CA relationships to either the activating or inhibiting term of the PN-Equation and to cope with the dose dependency of magnitude and frequency being either anabolic or catabolic, four sets of PN-Equations were required, where (i) both magnitude and frequency were anabolic, (ii) magnitude was anabolic and frequency catabolic, (iii) frequency anabolic and magnitude catabolic, and (iv) both magnitude and frequency were catabolic.

The solution to the PN-Equation provides a dimensionless value called "PN-Activity" that indicates the activation of a specific CA. Calculating the solution for each CA results in an overall cell (mRNA) profile, that is, interrelated CA in terms of the simulated mRNA expressions. The higher the value of a PN-Activity, the higher the activity of a NP cell to express the respective mRNA. A PN-Activity of 0 means minimal (and not "zero") expression of the respective mRNA.

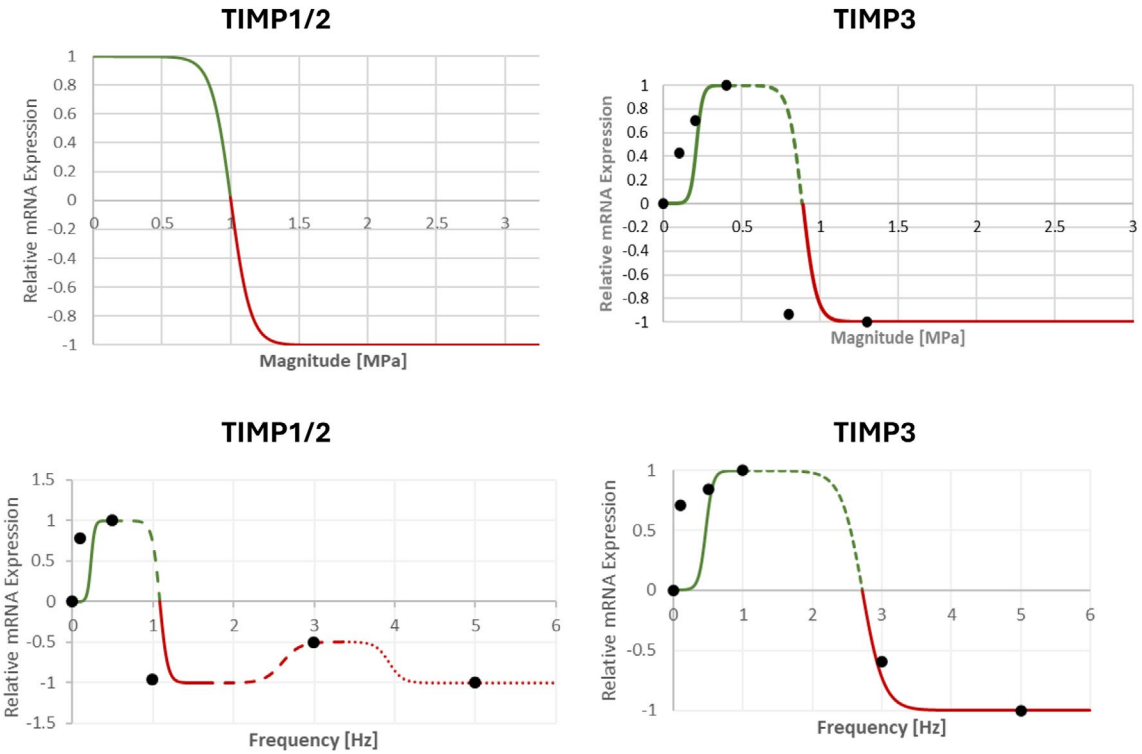

FIGURE 3 | Simulated response of TIMP to magnitude and frequency. Due to a lack of data, it was initially assumed that TIMP2 follows a similar behavior to TIMP1. The relationship of TIMP 1 and TIMP2 to magnitude is based on generic, knowledge-based assumptions [27]. Activating effect of loading on TIMP is reflected with values between 0 and 1 (green). Inhibiting effects of loading on TIMP is reflected by values between 0 and −1 (red).

2.3 | Application of the PN-Methodology on the Current System (Figure 1)

Functions that relate proteases and pro-inflammatory cytokines of NP cells to global stimuli (glucose, pH, magnitude, frequency) were used as previously discussed [27, 28] (Appendix S1). In contrast, all the data related to TIMP mRNA expressions were newly approximated and are subsequently introduced.

A data-driven approach was used to estimate the sensitivity of TIMP to glucose, pH, magnitude, and frequency, as exemplified in Figure 2. Experimental data from Gilbert and colleagues were used to estimate the relationship between pH and TIMP [23] and data from Saggese et al. [26] was used to estimate the relationship between glucose and TIMP1. The response of TIMP to magnitude and frequency was obtained from Li et al. [22]. Unfortunately, experimental data was only partially available. Hence, similarities among TIMP were examined to approximate missing data. Specifically, knowledge about selective protease inhibition, that is, TIMP1,2 rather than inhibiting MMP3 [11, 14] and TIMP3 rather than inhibiting ADAMTS4 [15], drove the decision to approximate missing TIMP2 information with TIMP1 data whenever TIMP1 data were available. An overview of all the experimental data used is provided in Appendix S1.

Functions that describe x_S^{TIMP} were fitted using the free online graphing calculator DESMOS (https://www.desmos.com/calculator). The parameters of a sigmoidal function were optimized to make the curve match the discrete data points from the experimental measurements. The curve-fitting approach was used as previously explained [28, 29].

To relate TIMP1 and TIMP2 mRNA expression to a physiological spectrum of magnitude, a generic function was used, as literature data report the largest apparent mRNA fold-change between 0.8 and 1.3 MPa in accordance with the profile of the generic function. Generic functions are knowledge-based functions that were built on a variety of experimental data and reflected an overall range within which a loading might be beneficial and in which range loading might be detrimental. For magnitude, a shift from beneficial to detrimental (for persisting/chronic pressure values) is roughly estimated to be around 1 MPa (see Section 3, Figure 3; for more information [27], Appendix S1).

Instructions on how to obtain weighting factors were previously provided [28]. In short, a maximum change in mRNA expression of cells exposed to different concentrations of stimuli (ϵ) was obtained from experimental research. To cope with the discrepancy between mRNA suppression (ranging from 0 to 1) and mRNA increase (ranging from $1 < \infty$), a function of ϵ ($f(\epsilon)$) was applied to turn mRNA suppression to semi bounded ranges by using reciprocal proportional relationships $f(\epsilon) = \epsilon$ and $f(\epsilon) = \frac{1}{\epsilon}$ for $\epsilon > 1$ and for $0 < \epsilon < 1$, respectively. Thereby, $f(\epsilon)$ was understood as an estimation of the "cellular effort" to increase or decrease mRNA expressions compared to a control. To calculate the weighting factors (θ_S^{CA}), $f(\epsilon)$ for all significant relationships were normalized to the highest $f(\epsilon)$ within the network, whereas nonsignificant S-CA relationships were set to a θ_S^{CA} of 0.0010 to be less than 5% of the lowest experimentally determined weighting factor (here, the relationship between pH and TIMP1 with 0.0339, see Section 3, Table 2). The respective θ_S^{CA} to estimate the effect of pro-inflammatory cytokines on TIMP were obtained from personal communication (Appendix S1).

TABLE 1 | Overview of stimulus values used to simulate five human habits within three nutrient environments.

Stimulus	Optimal		Critical	Early degenerated	
Glucose (mM)	5		1.03	0.89	
pH	7.1		6.95	6.93	
Stimulus	**Sitting**	**Walking**	**Hiking (+20 kg)**	**Jogging**	**Vibration**
Magnitude (MPa)	0.55	0.60	1.1	0.65	0.55
Frequency (Hz)	0.0001	1.80	1.00	2.75	15.00

TABLE 2 | Functions that relate the cell activity (CA) in terms of TIMP1, TIMP2, and TIMP3 mRNA expressions with varying physiological nutrient concentrations.

CA	x_S^{CA}	
TIMP1	$x_{glc}^{TIMP1} = \frac{e^{14.87*(glc)}}{e^{14.87*(glc)} + 2.979*10^{19}}$	$6.5 < pH \leq 7.0738$
		$x_{pH_1}^{TIMP1} = \frac{e^{-44.213*(pH-6.5)}}{e^{-44.213*(pH-6.5)} + 3.28*10^{-6}}$
		$7.0738 < pH \leq 7.4$
		$x_{pH_2}^{TIMP1} = \frac{e^{35.65*(pH-6.5)}}{e^{35.65*(pH-6.5)} + 2.62*10^{14}}$
	$x_{mag}^{TIMP1} = \frac{e^{14mag}*1.99999}{e^{14mag} + 1.2*10^{6}} - \frac{1.99999}{2}$	$0 \leq freq \leq 0.5005$
		$x_{freq_1}^{TIMP1} = \frac{e^{43.2*(freq)}}{e^{43.2*(freq)} + 2.128*10^{4}}$
		$0.5005 < freq \leq 1.0874$
		$x_{freq_2}^{TIMP1} = 1.99995 * \frac{-e^{21*(freq)}}{e^{21*(freq)} + 8.27*10^{9}} + 1$
		$1.0870 < freq \leq 1.62514$
		$x_{freq_3}^{TIMP1} = 1.99995 * \frac{-e^{21*(freq)}}{e^{21*(freq)} + 8.27*10^{9}} + 1$
		$1.62514 < freq < 3.3625$
		$x_{freq_4}^{TIMP1} = 0.5 * \frac{e^{9*(freq)}}{e^{9*(freq)} + 1.50*10^{10}} - 1$
		$3.3625 < freq \leq 40$
		$x_{freq_5}^{TIMP1} = 0.5 * \frac{-e^{12*(freq)}}{e^{12*(freq)} + 3.10*10^{20}} - 0.5$
TIMP2	glc, mag, freq: see TIMP1	$6.5 < pH \leq 6.8381$
		$x_{pH_1}^{TIMP2} = 0.46 * \frac{e^{40*(pH-6.5)}}{e^{40*(pH-6.5)} + 1.4*10^{3}}$
		$6.8381 < pH \leq 7.0604$
		$x_{pH_2}^{TIMP2} = 0.182 * \frac{e^{33.4*(pH-6.5)}}{e^{33.4*(pH-6.5)} + 1.0*10^{6}} + 0.438$
		$7.0604 < pH \leq 7.4$
		$x_{pH_3}^{TIMP2} = 0.40 * \frac{e^{35.3*(pH-6.5)}}{e^{35.3*(pH-6.5)} + 8.0*10^{9}} + 0.6$
TIMP3	glc: see TIMP1	$6.5 < pH \leq 6.8262$
	$0 \leq mag \leq 0.4096$	$x_{pH_1}^{TIMP3} = 0.99996 * \frac{e^{119.43*(pH-6.5)}}{e^{119.43*(pH-6.5)} + 0.52532}$
	$x_{mag_1}^{TIMP3} = \frac{e^{51*(mag)}}{e^{51*(mag)} + 4.0*10^{4}}$	$6.8262 < pH \leq 7.0267$
	$0.4096 < mag \leq 0.8871$	$x_{pH_2}^{TIMP3} \frac{e^{-137.38*(pH-6.5)}}{e^{-137.38*(pH-6.5)} + 1.3611*10^{-24}}$
	$x_{mag_2}^{TIMP3} = 2 * \frac{-e^{23*(mag)}}{e^{23*(mag)} + 7.278*10^{8}} + 1$	$7.0267 < pH \leq 7.4$
	$0.8871 < mag \leq 3.5$	$x_{pH_3}^{TIMP3} = \frac{e^{46.41*(pH-6.5)}}{e^{46.41*(pH-6.5)} + 1.1181*10^{18}}$
	$x_{mag_3}^{TIMP3} = 2 * \frac{-e^{23*(mag)}}{e^{23*(mag)} + 7.278*10^{8}} + 1$	$0 < freq \leq 0.99975$
		$x_{freq_1}^{TIMP3} = \frac{e^{19.5*(freq)}}{e^{19.5*(freq)} + 8*10^{3}}$
		$0.99975 < freq \leq 2.7200$
		$x_{freq_2}^{TIMP3} = 2 * \frac{e^{-6.51*(freq)}}{e^{-6.51*(freq)} + 2.04*10^{-8}} - 1$
		$2.7200 < freq \leq 5.0$
		$x_{freq_3}^{TIMP3} = 2 * \frac{e^{-6.51*(freq)}}{e^{-6.51*(freq)} + 2.04*10^{-8}} - 1$

Note: Glucose (glc): $0 < glc\ (mM) \leq 5.0$; pH: $6.5 < pH \leq 7.4$; magnitude (mag) $0 < mag\ (MPa) \leq 3.5$; frequency (freq); $0 < freq\ (Hz) \leq 40$. If several (n) functions were required to describe a physiological range, functions were indicated with a subscript, from 1 to n.

2.4 | Predicting a Pro-Inflammatory Environment

The protein levels of the pro-inflammatory cytokines, Y_{IL1B}, Y_{TNF}, were estimated based on their respective mRNA expressions (Equations 2 and 3): PN-Activities of IL1B and TNF ($\omega_{IL1B}, \omega_{TNF}$) were normalized by their respective maximum possible mRNA expression ($\omega_{IL1B,max}, \omega_{TNF,max}$). Maximum mRNA expressions were obtained by setting x_S^{CA} to a value of one under conditions that only activate the considered pro-inflammatory cytokine, that is, when the inhibition term of the PN-Equation is zero (see [27]).

$$Y_{IL1B} = \frac{\omega_{IL1B}}{\omega_{IL1B,max}} \tag{2}$$

$$Y_{TNF} = \frac{\omega_{TNF}}{\omega_{TNF,max}} \tag{3}$$

Y_{IL1B} and Y_{TNF} were then fed back into the intracellular network (Figure 1) as x_{IL1B}^{CA} and x_{TNF}^{CA}, respectively (see Figure 2, example for x_{TNF}^{TIMP1}) to calculate the mRNA expressions of TIMP1, TIMP2, TIMP3, MMP3, and ADAMTS4 of cells exposed to a pro-inflammatory environment.

2.5 | Simulated Conditions

PN-Activities for five daily human habits were simulated: "sitting," "walking," "hiking with 20kg extra weight," "jogging," and "exposure to high vibration." Human habits were chosen according to prolonged activities of humans where cells might adapt to input stimuli, including possibly critical activities such as "exposure to high vibration" and "hiking with 20 kg extra weight." Intradiscal pressures were obtained from in vivo measurements by Wilke et al. [21]. Frequencies for walking and jogging were obtained from the literature [32, 33]. A hiking pace of one step per second was assumed and a vibration frequency approximating an exposure to the vibration of an engine was reflected by a value of 15.00 Hz.

All the human habits were simulated for three nutritional conditions that were obtained from mechano-transport finite element (FE) models [34] (previously used as input for network modeling [28]). Two conditions simulated a non-degenerated IVD: one close to the Cartilage Endplates ("optimal" condition [30, 35]); one around the mid-transverse plane of the IVD, in the anterior region of the NP, where the most adverse nutrient conditions were found within the mechanically loaded disc ("critical" condition). A third nutritional condition reflected an IVD also around the anterior mid-transverse plane of the NP, with a simulated early degenerated Cartilage Endplate [28] ("early degenerated" condition) (Table 1).

3 | Results

3.1 | System Parameters

All the functions obtained to describe the response of TIMP to global stimuli are listed in Table 2.

A visualization of the responses of TIMP to magnitude and frequency is provided in Figure 3.

The most pronounced lack of data was found with respect to TIMP2, where protein-specific information was only found for its mRNA expression related to varying pH (Appendix S1).

The weighting factors for this system are given in Table 3. The strongest S-CA relationship within the PN-System was found to be the relationship between pH and IL1B.

3.2 | System Predictions

Cells not exposed to pro-inflammatory cytokines showed a high anabolic CA with elevated TIMP2 and TIMP3 mRNA expressions in all human habits throughout all nutrient conditions. TIMP1 only showed notable upregulation in "hiking with 20 kg extra weight." Elevated protease mRNA expression was only predicted for hiking with additional weight and vibration, while remaining minimal for any other condition. Exposure to pro-inflammatory cytokines had a marginal effect on TIMP but caused an upregulation of proteases in all the simulated conditions. Upregulation of MMP3 was more pronounced than the one of ADAMTS4 (Figure 4) and notably upregulated towards more adverse nutrient conditions.

In terms of pro-inflammatory cytokines, the mRNA expression of IL1B was predicted to be higher than the mRNA expression of TNF. PN-Activities of both IL1B and TNF slightly rose under more adverse nutrient concentrations (Figure 5, left). IL1B protein synthesis was overall constantly low throughout different nutrient and loading conditions, while TNF largely increased with adverse nutrient and loading conditions (Figure 5, right).

4 | Discussion

4.1 | TIMP and Protease Cell Profiles (Figure 4)

Unique TIMP and protease CA for a variety of human habits for three different nutrient concentrations were obtained for NP cells exposed and not exposed to pro-inflammatory cytokines. Such cell profiles provided by the PN-Methodology might be read as relative CA of one (average) cell, or they can be interpreted as the average response of various cells. This becomes particularly important when comparing simulation results with experimental data on the percentage of immunopositive cells for TIMP and proteases for different stages of degeneration [5], and with evaluations of the effect of a combined IL1B and TNF-enriched culture medium on bovine NP biopsies [36].

With more adverse nutrient concentrations, a catabolic shift was predicted, which is particularly pronounced in cells exposed to pro-inflammatory cytokines. The low effect of varying physiological and early degenerated nutrient concentrations within short timeframes agrees with general expectations that degenerative processes take months to years to evolve. However, the literature shows that with increasing degeneration

TABLE 3 | Weighting factos for each cell activity (CA) and stimulus (S) (θ_S^{CA}).

Stimulus	mRNA	θ_S^{CA}	Stimulus	mRNA	θ_S^{CA}
glc	MMP3	0.0010	mag	MMP3	0.0010
	ADAMTS4	0.0010		ADAMTS4	0.0494
	IL1B	0.0010		IL1B	0.0010*
	TNF	0.0010		TNF	0.0010*
	TIMP1	0.0010		TIMP1	0.0010
	TIMP2	0.0010*		TIMP2	0.0010*
	TIMP3	0.0010*		TIMP3	0.0694
pH	MMP3	0.3500	freq	MMP3	0.1852
	ADAMTS4	0.0704		ADAMTS4	0.0988
	IL1B	**1.0000**		IL1B	0.0010*
	TNF	0.0010		TNF	0.0010*
	TIMP1	0.0623		TIMP1	0.0353
	TIMP2	0.0417		TIMP2	0.0353*
	TIMP3	0.0010		TIMP3	0.0803
IL1B	MMP3	0.1333	TNF	MMP3	0.3310
	ADAMTS4	0.0010		ADAMTS4	0.0710
	TIMP1	0.0010*		TIMP1	0.0010*
	TIMP2	0.0010*		TIMP2	0.0010*
	TIMP3	0.0010		TIMP3	0.0010

Note: The highest weighting factor is shown in bold, weighting factors of nonsignificant S-CA relationships are set to 0.0010. S-CA relationships marked with asterisk symbol were not found in (or could not be directly translated from) the literature and an approximate weighting factor was assumed.
Abbreviations: Freq, frequency; Glc, glucose; Mag, magnitude.

grades, the relative percentage of cells immunopositive for pro-inflammatory cytokines also increases [16, 27]. Therefore, in addition to the individual catabolic shift of one cell, the number of cells showing catabolic activity also rises.

Regarding specific human movement habits, a strong catabolic shift due to exposure to vibration (15 Hz, Table 1) is in agreement with findings reporting that a low level of frequency is required to maintain the functionality of the IVD [22, 37, 38]. However, high vibration might often be damped, so that detrimental loading might not reach the NP cell microenvironment. Interestingly, an elevated TIMP1 expression was only predicted by the model for hiking with extra weight, the only condition that exceeds intradiscal loading pressure of 1 MPa (Table 1). This was supported by experimental findings that TIMP1 expressions in bovine NP tend to be upregulated under loading conditions exceeding 1 MPa [39].

As per pro-inflammatory cytokine exposure, the model predicts an overall catabolic shift (Figure 4), which is supported by various experiments [16, 28, 40, 41]. Thereby, the catabolic shift is characterized by a stagnant TIMP mRNA expression and a rise in proteases. Similar findings were provided for TIMP3, with a stagnant percentage of immunopositive cells, while the percentage of immunopositive cells of any other mRNA expressions tackled in this study significantly rose throughout degenerative stages [5]. A stagnant prediction of TIMP1 and TIMP2 is attributed to the lack of data about the relationship between IL1B and TNF on TIMP1 and TIMP2, which required the use of data of TIMP3 also for TIMP1 and TIMP2 (see also Appendices S1 and S2). As soon as experimental data about the individual effect of IL1B and TNF on TIMP1 and TIMP2 is available, the PN modeling design allows for a smooth implementation of this information.

Regarding proteases, a rise of MMP3 for all the human activities due to the presence of pro-inflammatory cytokines was predicted, which is in concordance with a positive correlation between increasing percentages of cells immunopositive for MMP3, degeneration grades [5] and correspondingly to combined IL1B and TNF exposure [36].

ADAMTS4 mRNA expression was predicted to be minimal and low, without and with pro-inflammatory cytokine exposure, respectively. This was confirmed by a nonsignificant change in ADAMTS4 expression due to combined IL1B and TNF exposure [36]. ADAMTS4 levels were, however, always increased under hiking with extra weight and with exposure to high vibration (Figure 4). This confirms that such loading conditions might contribute to IDD by reflecting detrimental effects as found in

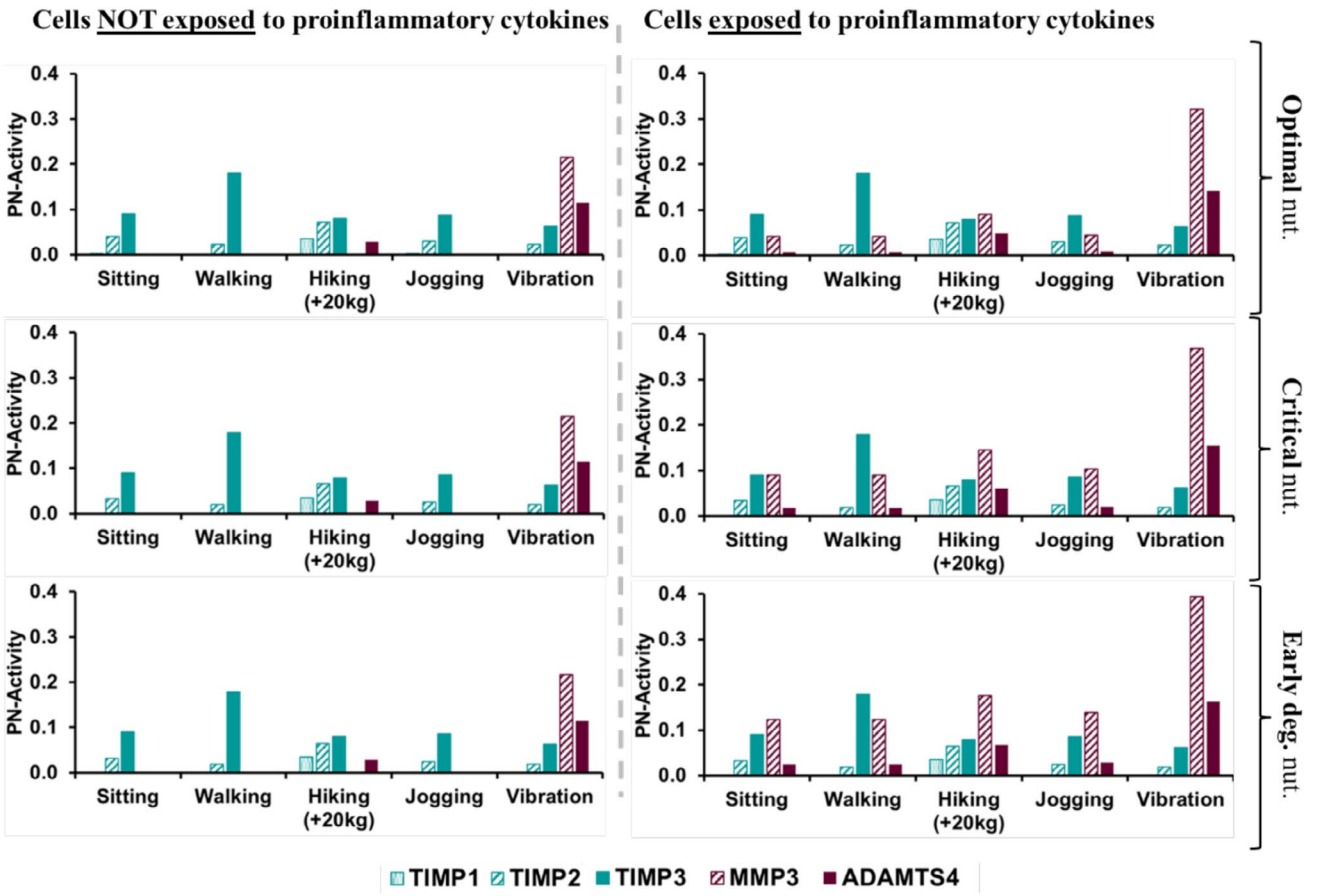

FIGURE 4 | Predicted mRNA profiles for cells not exposed and exposed to pro-inflammatory cytokines for five human habits: sitting, walking, hiking with 20 kg extra weight, jogging, and exposure to high vibration, and within three different nutrient (nut.) environments being optimal (pH 7.1, 5 mM glucose), critical (pH 6.95, 1.03 mM glucose), and early degenerated (pH 6.93, 0.89 mM glucose).

weight lifting, heavy work (carpenters) [42, 43] and whole body vibration (machine drivers) [43], respectively. Hence, results support the benefit of hip belts while hiking with extra load.

In terms of relative mRNA predictions within the cell profiles, TIMP3 mRNA expression was predicted by the model to be the most upregulated TIMP mRNA expression, independently of the presence of pro-inflammatory cytokines. This goes along with findings by Le Maitre et al. [5], who observed that throughout degeneration, TIMP3 immunopositivity was always highest compared to TIMP1 and TIMP2 immunopositivity. Thereby, a rise of TIMP2 was only found for importantly degenerated IVD, which goes along with our findings that only encompass early degenerative states (see Section 4.2 for relativization). However, a rise of TIMP1 immunopositivity was already observed at lower degenerative states [5], which might suggest an underprediction of TIMP1 by the model at early-degenerative nutrient concentration. Conversely, other experimental studies regarding the effect of TIMP1 on TNF and IL1B on bovine whole organ cultures confirmed nonsignificant alterations of TIMP1 within combined TNF and IL1B exposure for up to 7 days of exposure, before becoming significant [36]. Such findings emphasize the importance of time sensitivity to duly categorize and understand CA in both experimental and in silico research. While the effect of long-term exposure is yet to be fully investigated for the current TIMP and protease regulations, the PN-Methodology was designed for the continuous integration of time-sensitive approximations [27] and can, thus, eventually provide more insight into temporal considerations.

In terms of proteases, MMP3 immunopositivity was predicted by the model to be minimal in the absence of pro-inflammatory cytokines for all non-catabolic loading conditions. This is aligned with negligible MMP3 immunopositivity in non-degenerated NP cells [5]. However, the overall low ADAMTS4 mRNA expression stood in contrast to the findings of Le Maitre and colleagues [5], who found that around 20% of NP cells expressed ADAMTS4 already at a non-degenerative state, which then rises throughout degeneration. This indicates that changes in ADAMTS4 might be correctly predicted by the model, whilst the overall PN-Activity compared to other mRNA expressions might be underpredicted. Reasons for this might be important discrepancies between the used experimental data (Appendix S1) and actual human in vivo expressions or the neglect of an additional (global) stimulus that strongly regulates ADAMTS4 mRNA expression, in addition to the four tackled global stimuli. This outcome shows the potential of the PN approach to identify whether key relevant stimuli were considered for a certain mRNA expression.

Indeed, the direct use of experimental data enabled by the PN modeling approach allows to maintain the model close to biological finding and is, thus, beneficial. However, this goes along with three main types of assumptions because of limited data availability and non-standardized experimental protocols: (i) a

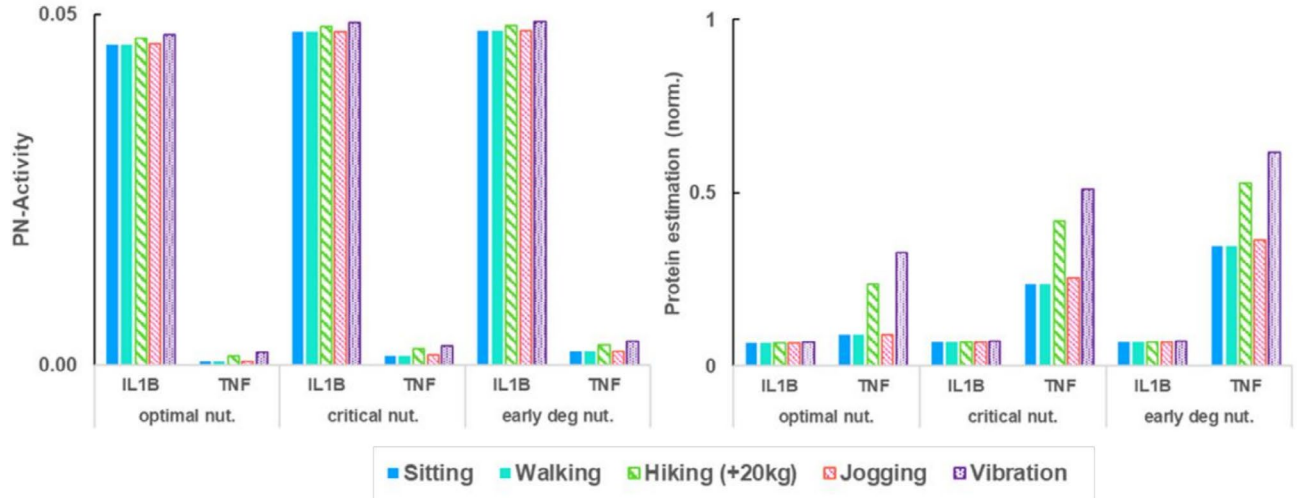

FIGURE 5 | mRNA expressions (left) and protein estimations (right) of TNF and IL1B under different nutritional (nut.) and loading conditions.

lack of information for the mathematical functions, (ii) the need for pooling together primary cell cultures from different species and different culture conditions, and (iii) a lack of evidence-based mathematical models to pass from mRNA expression to protein secretion (Section 4.2). In the present model, unfortunately, experimental data for TIMP2 was only available regarding pH. Missing information on TIMP2 mRNA expression upon glc, mag, and freq variations was approximated with the corresponding responses reported for TIMP1. This decision was based on the similarity of the selective binding of TIMP1 and TIMP2 to MMP3 [11, 14] (see Section 2). For an optimal prediction of TIMP2 mRNA expression, experiments should expose NP cell cultures to varying levels of glc, mag, or freq. Stimuli should optimally cover physiologically relevant ranges of stimulations (see Secstion 2.2 and Figures 1 and 2). Particularly for mechanical loading, full ranges are not always given (e.g., [37]), which may lead to an underestimation of the impact of that stimulus on a CA. Additionally, information about TIMP mRNA expression upon exposure of NP cells to pro-inflammatory cytokines was generally limited, and TIMP3-like impact was assumed for both TIMP1 and TIMP2.

As a lack of data is a common problem in biological network modeling, the PN-Methodology was specifically designed to offer the following advantages in its quality as a high-level approach: (i) it requires a reduced amount of experimental data compared to intracellular network models; (ii) it permits straightforward substitution and aggregation of experimental data. Hence, by the way it is built, the model can improve as further data is produced. It is, thus, a great tool to progressively integrate new data and to suggest the need for new specific experiments, even if early versions unavoidably suffer limitations because of the data-driven nature of the functions and the theta values. Extensive information about the source of the data and corresponding limitations, such as an overview of the strength of the experimental basis for the current results, is given in Appendices S1 and S2.

Despite its limitations, this model was able to provide valuable semi-quantitative predictions as per pro-anabolic or pro-catabolic cell states, which was demonstrated through qualitative comparisons with literature data and knowledge. Given that a wide variation of cell culture models exists, and experimentalists generally have a limited control over the control groups and the conditioning of cell perturbations, quantitative validations could only be done with consistent sets of primary cells cultured under all the conditions explored in the model. Unfortunately, such data do not exist at the present time to the best of our knowledge. Hence, qualitative validation of the type of CA and robustness against falsification tests remained the best options. However, as a future development, we shall consider replacing the fitted functions with Bayesian interpolations to include the stochastic aspects of the data we are using.

Eventually, to evaluate the inhibitory potential of TIMP on proteases arising from the presented cell profiles, further analysis was conducted (Appendix S3), predicting TIMP to efficiently downregulate proteases in all conditions but exposure to vibration in cells not exposed to pro-inflammatory cytokines. Due to pro-inflammatory cytokine exposure, particularly the inhibition of MMP3 was predicted to be impeded.

4.2 | The Pro-Inflammatory Environment (Figure 5)

At the mRNA level, both IL1B and TNF were predicted to have a relatively low expression with a PN-Activity of less than 0.05; thereby, IL1B was expressed more highly than TNF. This tendency was also found in experimental research, where both the percentage of cells that express IL1B and its receptor tended to be higher than the percentage of cells that express TNF and its receptor [16]. Interestingly, the translation to proteins through the PN-Methodology indicated that, particularly under critical and early degenerated nutritional conditions, the catabolic shift of pro-inflammatory cell profiles (Figure 4, right) was provoked by an increase of TNF, rather than of IL1B proteins. This finding is biologically interesting, related to the generally assumed detrimental effect of TNF [18], in contrast to a possible physiological role of IL1B at low concentrations [44].

Given that the PN-Methodology only describes relative changes of a CA, a baseline of pro-inflammatory cytokine levels under

physiological concentrations would be required to further evaluate model predictions. In other words, measurements would be required to contrast quantitative IL1B and TNF protein levels under non-degenerated and early degenerated conditions. In terms of quantity, however, only a few studies actually investigated physiological cytokine expression within IVD tissue [45–47]. Importantly, those studies suggest that pro-inflammatory cytokine levels range within pg/mL, whereas most experimental studies focusing on the effect of pro-inflammatory cytokines, including the ones used for this study (Appendix S1), stimulate cell cultures with around 10 ng/mL, which seems to be largely hyper-physiological. In contrast, experimental studies simulating mechanical or nutritional environments are often stimulated under physiological conditions (see, e.g., studies listed in Appendix S1). This bias is translated into in silico research and, consequently, the hereby presented model predictions of the pro-inflammatory status might be biased or possibly reflect higher degenerative states in terms of pro-inflammatory environments than early degeneration. Moreover, this current work considers a linear relationship between mRNA expression and protein synthesis, neglecting possible posttranscriptional regulations because of a lack of experimental knowledge. Posttranscriptional mechanisms can be highly complex. Yet, should matching sets of mRNA expression and secretoma proteomics data become available for NP cell cultures, the most relevant correlations and corresponding mathematical functions might be explored for further integration in the current PN-Methodology. Further discussion focused on mathematical aspects of the PN-Methodology are provided in Appendix S2.

Overall, the PN-Methodology provides a phenomenological novel systems biology network modeling approach that aims to simulate effective CA in response to multifactorial environments. It was shown hereby that the PN-Methodology provides estimations of TIMP, proteases, and pro-inflammatory cytokines in accordance with a broad spectrum of literature evidence. Simulated CA could be used to create biological risk indexes for IVD degeneration, thanks to couplings with FE models that integrate patient-specific IVD morphologies [48, 49]. In particular, mechano-transport FE models control local internal mechanical loads, glucose concentration, and pH [34, 48]. Once personalized with medical images, such models would provide PN models with sufficient input to achieve simulation-based biological risk factors in terms of pro-anabolic or pro-catabolic CAs, which could benefit advanced patient stratification.

5 | Conclusions

This work aimed to provide insight into the dynamics of TIMP, proteases, and pro-inflammatory cytokines in response to the multifactorial NP environment. Approximations were obtained through the PN-Methodology, which was used (i) to estimate relative mRNA expressions of TIMP and proteases and (ii) to approximate a pro-inflammatory environment. Predicted cell responses largely agree with independent experimental studies, indicating that the PN-Methodology proves utility in estimating CA in response to complex stimulus environments. The strength of the PN-Methodology is its efficiency in comprehensively estimating CA in complex multifactorial environments, without the need to simulate intracellular regulatory networks. Coupled with patient-specific mechano-transport FE models, it paves the way towards advanced patient stratification in terms of biological risk factors for IVD degeneration.

Further work should investigate the generalization of this methodology toward other tissues, its validity to link mRNA expressions with corresponding protein synthesis, and possibly a more stochastic approach for data integration.

Author Contributions

Study concept and design: L. Baumgartner and J. Noailly. Acquisition of material and data: S. Witta and L. Baumgartner. Data analysis: S. Witta and L. Baumgartner. Preparation of the manuscript: L. Baumgartner. Critical reviewing and approval of the manuscript: all authors.

Acknowledgments

The authors thank Paola Bermudez for providing information about her cell culture experiments within the framework of disc4all (Disc4All-MSCA-2020-ITN-ETN 955735) regarding the response of TIMP3 to IL1B and TNF-enriched culture media. This work was financially supported by the European Research Council (ERC-2021-CoG-O-Health-101044828).

Conflicts of Interest

The authors declare no conflicts of interest.

Data Availability Statement

All the functions (x_S^{CA}) and values of the weighting factors (θ_S^{CA}) are provided within this work or within previous open access publications. The methodology on how to build PN-Equations is provided within this work and more extensively in previous work [27]. Additionally, we are working on curating the full code for online redistribution, which shall be ready by the time of the review.

References

1. D. Hoy, L. March, and P. Brooks, "The Global Burden of Low Back Pain: Estimates From the Global Burden of Disease 2010 Study," *Annals of the Rheumatic Diseases* 73, no. 6 (2014): 968–974, https://doi.org/10.1136/annrheumdis-2013-204428.

2. T. Vos, C. Allen, and M. Arora, "Global, Regional, and National Incidence, Prevalence, and Years Lived With Disability for 310 Diseases and Injuries, 1990–2015: A Systematic Analysis for the Global Burden of Disease Study 2015," *Lancet* 388, no. 10053 (2016): 1545–1602, https://doi.org/10.1016/S0140-6736(16)31678-6.

3. L. J. Smith, N. L. Nerurkar, K. S. Choi, B. D. Harfe, and D. M. Elliott, "Degeneration and Regeneration of the Intervertebral Disc: Lessons From Development," *Disease Models & Mechanisms* 4 (2011): 31–41, https://doi.org/10.1242/dmm.006403.

4. F. J. Lyu, H. Cui, H. Pan, et al., "Painful Intervertebral Disc Degeneration and Inflammation: From Laboratory Evidence to Clinical Interventions," *Bone Research* 9 (2021): 7, https://doi.org/10.1038/s41413-020-00125-x.

5. C. L. Le Maitre, A. J. Freemont, and J. A. Hoyland, "Localization of Degradative Enzymes and Their Inhibitors in the Degenerate Human Intervertebral Disc," *Journal of Pathology* 204 (2004): 47–54, https://doi.org/10.1002/path.1608.

6. A. J. Pockert, S. M. Richardson, C. L. le Maitre, et al., "Modified Expression of the ADAMTS Enzymes and Tissue Inhibitor of

Metalloproteinases 3 During Human Intervertebral Disc Degeneration," *Arthritis and Rheumatism* 60 (2009): 482–491, https://doi.org/10.1002/art.24291.

7. J. Daniels, A. A. L. Binch, and C. L. le Maitre, "Inhibiting IL-1 Signaling Pathways to Inhibit Catabolic Processes in Disc Degeneration," *Journal of Orthopaedic Research* 35 (2017): 74–85, https://doi.org/10.1002/jor.23363.

8. M. D. Tortorella, M. Pratta, R. Q. Liu, et al., "Sites of Aggrecan Cleavage by Recombinant Human Aggrecanase-1 (ADAMTS-4)," *Journal of Biological Chemistry* 275 (2000): 18566–18573, https://doi.org/10.1074/jbc.M909383199.

9. L. Baumgartner, K. Wuertz-Kozak, C. L. le Maitre, et al., "Multiscale Regulation of the Intervertebral Disc: Achievements in Experimental, In Silico, and Regenerative Research," *International Journal of Molecular Sciences* 22 (2021): 22703, https://doi.org/10.3390/ijms22020703.

10. M. H. Lee, S. Atkinson, and G. Murphy, "Identification of the Extracellular Matrix (ECM) Binding Motifs of Tissue Inhibitor of Metalloproteinases (TIMP)-3 and Effective Transfer to TIMP-1," *Journal of Biological Chemistry* 282, no. 9 (2007): 6887–6898, https://doi.org/10.1074/jbc.M610490200.

11. M. Kashiwagi, M. Tortorella, H. Nagase, and K. Brew, "TIMP-3 Is a Potent Inhibitor of Aggrecanase 1 (ADAM-TS4) and Aggrecanase 2 (ADAM-TS5)*," *Journal of Biological Chemistry* 276 (2001): 12501–12504, https://doi.org/10.1074/jbc.C000848200.

12. F.-X. Gomis-Rüth, K. Maskos, and M. Betz, "Mechanism of Inhibition of the Human Matrix Metalloproteinase Stromelysin-1 by TIMP-1," *Nature* 389 (1997): 77–81, https://doi.org/10.1038/37995.

13. C. S. Moore and S. J. Crocker, "An Alternate Perspective on the Roles of TIMPs and MMPs in Pathology," *American Journal of Pathology* 180, no. 1 (2012): 12–16, https://doi.org/10.1016/j.ajpath.2011.09.008.

14. L. Costanzo, B. Soto, R. Meier, et al., "The Biology and Function of Tissue Inhibitor of Metalloproteinase 2 in the Lungs," *Pulmonary Medicine* 2022 (2022): 1–12, https://doi.org/10.1155/2022/3632764.

15. L. Troeberg, K. Fushimi, S. D. Scilabra, et al., "The C-Terminal Domains of ADAMTS-4 and ADAMTS-5 Promote Association With N-TIMP-3," *Matrix Biology* 28 (2009): 463–469, https://doi.org/10.1016/j.matbio.2009.07.005.

16. C. L. Le Maitre, J.A. Hoyland, A. J. Freemont, Catabolic Cytokine Expression in Degenerate and Herniated Human Intervertebral Discs: IL-1beta and TNFα Expression Profile," *Arthritis Research and Therapy* 9 (2007): R77, https://doi.org/10.1186/ar2275.

17. M. V. Risbud and I. M. Shapiro, "Role of Cytokines in Intervertebral Disc Degeneration: Pain and Disc Content," *Nature Reviews Rheumatology* 10, no. 1 (2013): 44–56, https://doi.org/10.1038/nrrheum.2013.160.

18. D. Purmessur, B. A. Walter, P. J. Roughley, D. M. Laudier, A. C. Hecht, and J. Iatridis, "A Role for TNFα in Intervertebral Disc Degeneration: A Non-Recoverable Catabolic Shift," *Biochemical and Biophysical Research Communications* 433 (2013): 151–156, https://doi.org/10.1016/j.bbrc.2013.02.034.

19. D. Mokhbi Soukane, A. Shirazi-Adl, and J. P. G. Urban, "Computation of Coupled Diffusion of Oxygen, Glucose and Lactic Acid in an Intervertebral Disc," *Journal of Biomechanics* 40 (2007): 2645–2654, https://doi.org/10.1016/j.jbiomech.2007.01.003.

20. J. P. G. Urban, S. Smith, and J. C. T. Fairbank, "Nutrition of the Intervertebral Disc," *Spine* 29 (2004): 2700–2709.

21. H. J. Wilke, P. Neef, M. Caimi, et al., "New In Vivo Measurements of Pressures in the Intervertebral Disc in Daily Life," *Spine* 24, no. 8 (1999): 755–762, https://doi.org/10.1097/00007632-199904150-00005.

22. P. Li, Y. Gan, H. Wang, et al., "Dynamic Compression Effects on Immature Nucleus Pulposus: A Study Using a Novel Intelligent and Mechanically Active Bioreactor," *International Journal of Medical Sciences* 13 (2016): 225–234, https://doi.org/10.7150/ijms.13747.

23. H. T. J. Gilbert, N. Hodson, P. Baird, S. M. Richardson, and J. A. Hoyland, "Acidic pH Promotes Intervertebral Disc Degeneration: Acid-Sensing Ion Channel −3 as a Potential Therapeutic Target," *Scientific Reports* 6 (2016), https://doi.org/10.1038/srep37360.

24. M. Huang, H. Q. Wang, Q. Zhang, X. D. Yan, M. Hao, and Z. J. Luo, "Alterations of ADAMTSs and TIMP-3 in Human Nucleus Pulposus Cells Subjected to Compressive Load: Implications in the Pathogenesis of Human Intervertebral Disc Degeneration," *Journal of Orthopaedic Research* 30 (2012): 267–273, https://doi.org/10.1002/jor.21507.

25. T. Handa, H. Ishihara, H. Ohshima, R. Osada, H. Tsuji, and K. Obata, "Effects of Hydrostatic Pressure on Matrix Synthesis and Matrix Metalloproteinase Production in the Human Lumbar Intervertebral Disc," *Spine* 22 (1997): 1085–1091, https://doi.org/10.1097/00007632-199705150-00006.

26. T. Saggese, A. Thambyah, K. Wade, et al., "Differential Response of Bovine Mature Nucleus Pulposus and Notochordal Cells to Hydrostatic Pressure and Glucose Restriction," *Cartilage* 11, no. 2 (2018): 221–233, https://doi.org/10.1177/1947603518775795.

27. L. Baumgartner, "Parallel Networks to Simulate Complex Multicellular Dynamics – A Proof of Concept With Intervertebral Disc Cell Systems," *bioRxiv* (2024): 2022.08.08.503195, https://doi.org/10.1101/2022.08.08.503195.

28. L. Baumgartner, A. Sadowska, L. Tío, M. A. González Ballester, K. Wuertz-Kozak, and J. Noailly, "Evidence-Based Network Modelling to Simulate Nucleus Pulposus Multicellular Activity in Different Nutritional and Pro-Inflammatory Environments," *Frontiers in Bioengineering and Biotechnology* 9 (2021), https://doi.org/10.3389/fbioe.2021.734258.

29. L. Baumgartner, J. J. Reagh, M. A. González Ballester, and J. Noailly, "Simulating Intervertebral Disc Cell Behaviour Within 3D Multifactorial Environments," *Bioinformatics* 37 (2021): 1246–1253, https://doi.org/10.1093/bioinformatics/btaa939.

30. C. Rinkler, F. Heuer, M. T. Pedro, et al., "Influence of Low Glucose Supply on the Regulation of Gene Expression by Nucleus Pulposus Cells and Their Responsiveness to Mechanical Loading," *Journal of Neurosurgery: Spine* 13, no. 4 (2010): 535–542, https://doi.org/10.3171/2010.4.spine09713.

31. A. Nachemson and G. Elfström, "Intravital Dynamic Pressure Measurements in Lumbar Discs," *Scandinavian Journal of Rehabilitation and Medication* 1 (1970): 1–40.

32. A. Pachi and T. Ji, "Frequency and Velocity of People Walking," *Structural Engineering* 84, no. 3 (2005): 36–40.

33. G. Vernillo, M. Giandolini, W. B. Edwards, et al., "Biomechanics and Physiology of Uphill and Downhill Running," *Sports Medicine* 47 (2017): 615–629, https://doi.org/10.1007/s40279-016-0605-y.

34. C. Ruiz Wills, B. Foata, M. Á. González Ballester, J. Karppinen, and J. Noailly, "Theoretical Explorations Generate New Hypotheses About the Role of the Cartilage Endplate in Early Intervertebral Disk Degeneration," *Frontiers in Physiology* 9 (2018), https://doi.org/10.3389/fphys.2018.01210.

35. A. Nachemson, "Intradiscal Measurements of Ph in Patients With Lumbar Rhizopathies," *Acta Orthopaedica Scandinavica* 40, no. 1 (1969): 23–42, https://doi.org/10.3109/17453676908989482.

36. O. Krupkova, M. Hlavna, J. Amir Tahmasseb, et al., "An Inflammatory Nucleus Pulposus Tissue Culture Model to Test Molecular Regenerative Therapies: Validation With Epigallocatechin 3-Gallate," *International Journal of Molecular Sciences* 17 (2016): 1640, https://doi.org/10.3390/ijms17101640.

37. J. J. MacLean, C. R. Lee, M. Alini, et al., "Anabolic and Catabolic mRNA Levels of the Intervertebral Disc Vary With the Magnitude and Frequency of In Vivo Dynamic Compression," *Journal of Orthopaedic Research* 22, no. 6 (2004): 1193–1200, https://doi.org/10.1016/j.orthres.2004.04.004.

38. J. J. MacLean, C. R. Lee, S. Grad, K. Ito, M. Alini, and J. C. Iatridis, "Effects of Immobilization and Dynamic Compression on Intervertebral Disc Cell Gene Expression In Vivo," *Spine* 28 (2003): 973–981, https://doi.org/10.1097/01.brs.0000061985.15849.a9.

39. C. L. Korecki, J. J. MacLean, and J. C. Iatridis, "Characterization of an In Vitro Intervertebral Disc Organ Culture System," *European Spine Journal* 16 (2007): 1029–1037, https://doi.org/10.1007/s00586-007-0327-9.

40. C. A. Séguin, R. M. Pilliar, P. J. Roughley, and R. A. Kandel, "Tumor Necrosis Factor-Alpha Modulates Matrix Production and Catabolism in Nucleus Pulposus Tissue," *Spine* 30 (2005): 1940–1948, https://doi.org/10.1097/01.brs.0000176188.40263.f9.

41. J. Wang, Y. Tian, K. L. E. Phillips, et al., "Tumor Necrosis Factor α- and Interleukin-1β-Dependent Induction of CCL3 Expression by Nucleus Pulposus Cells Promotes Macrophage Migration Through CCR1," *Arthritis and Rheumatism* 65 (2013): 832–842, https://doi.org/10.1002/art.37819.

42. T. Videman, S. Sarna, M. C. Battié, et al., "The Long-Term Effects of Physical Loading and Exercise Lifestyles on Back-Related Symptoms, Disability, and Spinal Pathology Among Men," *Spine* 20 (1995): 699–709, https://doi.org/10.1097/00007632-199503150-00011.

43. K. Luoma, P. Lama, U. Zehra, et al., "Why Do Some Intervertebral Discs Degenerate, When Others (In the Same Spine) do Not?," *Clinical Anatomy* 28, no. 2 (2014): 195–204, https://doi.org/10.1002/ca.22404.

44. K. L. E. Phillips, K. Cullen, N. Chiverton, et al., "Potential Roles of Cytokines and Chemokines in Human Intervertebral Disc Degeneration: Interleukin-1 Is a Master Regulator of Catabolic Processes," *Osteoarthritis and Cartilage* 23 (2015): 1165–1177, https://doi.org/10.1016/j.joca.2015.02.017.

45. H. Takahashi, T. Suguro, Y. Okazima, M. Motegi, Y. Okada, and T. Kakiuchi, "Inflammatory Cytokines in the Herniated Disc of the Lumbar Spine," *Spine* 21 (1996): 218–224.

46. R. Gawri, D. H. Rosenzweig, E. Krock, et al., "High Mechanical Strain of Primary Intervertebral Disc Cells Promotes Secretion of Inflammatory Factors Associated With Disc Degeneration and Pain," *Arthritis Research & Therapy* 16 (2014): R21, https://doi.org/10.1186/ar4449.

47. J. Zou, Y. Chen, J. Qian, and H. Yang, "Effect of a Low-Frequency Pulsed Electromagnetic Field on Expression and Secretion of IL-1β and TNF-α in Nucleus Pulposus Cells," *Journal of International Medical Research* 45 (2017): 462–470, https://doi.org/10.1177/0300060516683077.

48. A. Malandrino, J. M. Pozo, I. Castro-Mateos, et al., "On the Relative Relevance of Subject-Specific Geometries and Degeneration-Specific Mechanical Properties for the Study of Cell Death in Human Intervertebral Disk Models," *Frontiers in Bioengineering and Biotechnology* 3 (2015), https://doi.org/10.3389/fbioe.2015.00005.

49. E. Muñoz-Moya, M. Rasouligandomani, C. Ruiz Wills, F. K. Chemorion, G. Piella, and J. Noailly, "Unveiling Interactions Between Intervertebral Disc Morphologies and Mechanical Behavior Through Personalized Finite Element Modeling," *Frontiers in Bioengineering and Biotechnology* 12 (2024), https://doi.org/10.3389/fbioe.2024.1384599.

Supporting Information

Additional supporting information can be found online in the Supporting Information section.